Proceedings of the 28th IEEE
EMBS Annual International Conference
New York City, USA, Aug 30-Sept 3, 2006

AUTOMATIC MEDICAL IMAGE SEGMENTATION USING GRADIENT AND INTENSITY COMBINED LEVEL SET METHOD

Shaojun Liu and Jia Li

Abstract— **This paper presents a new level set based solution for automatic medical image segmentation. Study shows that level set methods using image intensity or gradient information alone can not generate satisfying segmentation on some complex organic structures, such as lung bronchia or nodules. We investigate the intensity distribution of these organic structures, and propose a calibrating mechanism to automatically weight image intensity and gradient information in the level set speed function. The new method can tolerate estimation error in intensity distribution and detect object boundaries whose gradient is low. The experimental results show that the proposed method gives stable and accurate segmentation results on public lung image data.**

I. INTRODUCTION

Propelled by growing computing power, 3D image processing techniques find increasing applications in medical domain, such as computer aided diagnose (CAD) and computer aided surgery. As a key technology, 3D image segmentation became a popular topic of medical image processing. Accurate 3D geometric information of organic structures is crucial for early disease diagnose and treatment. However, segmentation of some organic structures, such as lung bronchia and nodules, is a challenging task due to their complex topologies. This paper proposes a new automatic 3D image segmentation method for these structures based on level set method.

Level set method, proposed by Osher and Sethian, has been extensively studied and widely used in image segmentation [1]. Many variations have been proposed for improving the level set method. One branch of level set methods, fused the various regional statistics like intensity distribution, can enhance segmentation capabilities. For example, Baillard et al. incorporated pixel-classification based on intensity distribution into the level set speed function [2]. Their automatic method gave impressive segmentation results on brain images. To estimate distribution of incomplete data, Dempster et al. proposed an expectation-maximization (EM) framework [3], which has been adopted in many later approaches such as [4]. And a stochastic EM (SEM) algorithm, was proposed by Masson and Pieczynski to reduce the dependence on initialization of the EM method [5]. However, both the EM and SEM method do not guarantee the global optimal estimation and the estimation results depend on initialization. The estimation error in intensity distribution can make segmentation results instable as shown in the later sections of this paper. We investigate the effects of the estimation error and propose a new calibrating mechanism to combine gradient information and intensity distribution into segmentation process. By searching the maximal overlap of image gradient with the boundaries determined by intensity distribution, the proposed method can locate the boundaries of interested objects more stably.

The paper is organized as following. In Section II, we briefly describe the background of level set method and discuss the defects with segmentation by only image gradient or intensity distribution. Section III illustrates the new mechanism to combine gradient information and intensity distribution in segmentation. Experimental results are presented in Section IV. Section V concludes the paper and discusses future research directions.

II. BACKGROUND

The central idea of level set is to represent boundaries of different regions by a moving front $\gamma(t)$, which converges to the desired boundaries from its initial position. The moving front $\gamma(t)$ is a zero level set of a higher dimensional function $\psi(x,t), x \in \Re^N$, and represents a closed hyper-surface. It is propagated along its normal direction by updating $\psi(x,t)$ according to some criteria. The $\Re^N$space is then divided by the moving front, into the region Ω enclosed by $\gamma(t)$ and the outside region $\overline{\Omega}$, which satisfy: $\psi(x,t) < 0, x \in \Omega; \psi(x,t) = 0, x \in \gamma(t); \psi(x,t) > 0, x \in \overline{\Omega}$. The evolution equation for $\psi(x,t)$ is given as

$$\psi_t + F|\nabla\psi| = 0, \tag{1}$$

where F is the speed function of the moving front. A typical speed function is in the form of:

$$F = \hat{k}_I(F_A + F_G), \tag{2}$$

where $\hat{k}_I = 1/(1 + |\nabla G_\sigma * I(x)|^m)$ reflects the stopping criteria by image gradient, F_A is an advection term independent of the moving front's geometry, and F_G is a speed term dependent on the geometry such as local curvature.

The speed function should decrease to zero quickly when the front meets object boundaries. It suggests a large m in $\hat{k}_I$ if using image gradient as the only stopping criteria. Nevertheless, with a large m the front is likely to stop at regions with middle gradient, which may be noise or textures, instead of object boundaries in an image. On the other side, with a small m level set may leak into object boundaries whose gradient is low.

S. Liu is a Ph.D. Candidate in the department of Computer Science and Engineering, Oakland University, Rochester, MI 48309, USA sliu2@oakland.edu

J. Li is with the department of Computer Science and Engineering, Oakland University, Rochester, MI 48309, USA li4@oakland.edu

1-4244-0033-3/06/$20.00 ©2006 IEEE.

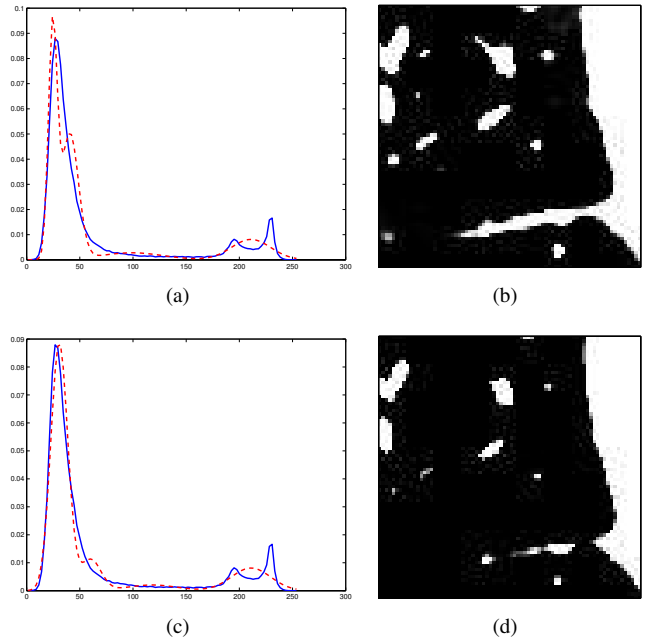

(a) (b) (c) (d)

Fig. 1. Instable segmentation results in (b) and (d), resulted from Two estimation of intensity distribution of a 3D image in (a) and (c) respectively. The blue line is the intensity histogram while red line the estimation result.

Using intensity distribution into the level set speed function, instead of image gradient, eliminates the need to adjust m, thus makes segmentation automatic. It can detect object boundaries with low gradient or reduce noise effect in gradient. However, an accurate and stable estimation of intensity distribution is difficult to get from a finite set of 3D image data. The EM or SEM method does not guarantee convergence, or find the global optimum, whose results depend on the initialization. Consequently, the segmentation result based on intensity distribution may be instable. For example, by running the SEM algorithm twice on a 3D lung image of size $80 \times 80 \times 28$, we get two estimation results of its intensity distribution, as shown in Fig. 1(a) and 1(c). Note the estimation results around the left peak are different in the two figures. Fig. 1(b) and 1(d) show the corresponding results of the level set segmentation on a slice at $z = 10$. The inside region in Fig. 1(d) "shrinks" compared with that in Fig. 1(b), resulting some structures to break or disappear. The original image of the slice and its gradient are shown in Fig. 2(a) and Fig. 2(b) for reference. Checking intensity values of different parts in Fig. 1, we find the left peak corresponds largely to the background, the right two peaks corresponding to lung walls, and the middle flat part corresponding to the organic structures we are interested on, such as bronchia, vessels and the boundaries of lung walls. As their intensity values are not distinctive from those of the background, a small disturbance on the estimation result of intensity distribution, will change the segmentation result of the low intensity structures obviously.

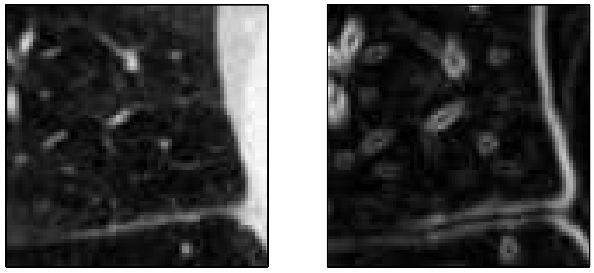

(a) Original Image (b) Gradient

Fig. 2. One slice at $z = 10$ in the 3D image in Fig. 1.

III. SEGMENTATION

To reduce the "shrink" or "expand" effect on segmentation results, we propose to use gradient information to calibrate the estimation of intensity distribution in the following. We compute the overlap of image gradient with the boundaries determined by intensity distribution through introducing a probability offset to intensity distribution. The maximum overlap indicates the optimal boundaries of the interested objects.

To restate the problem without losing generality, here we use a mixed Gaussian distribution model,

$$P(u) = \sum_{k=1}^{n} \pi_k P(u\,|\lambda_k; \mu_k, \sigma_k\,), \tag{3}$$

where π_k is the prior probability of class λ_k with $\sum_{k=1}^{n} \pi_k = 1$, and μ_k, σ_k are the mean and variance of the Gaussian distribution of the intensity. We then get the intensity distribution inside the region Ω,

$$P_{in}(u) = \sum_{k|\lambda_k \in \Omega} \pi_k P(u\,|\lambda_k; \mu_k, \sigma_k)\,. \tag{4}$$

And the intensity distribution of the outside region $\overline{\Omega}$, $P_{out}(u)$, can be obtained in a similar way. Normally for pixel x on region boundaries with $u = I(x)$, we have

$$P_{out}(I(x)) - P_{in}(I(x)) = 0. \tag{5}$$

The final boundaries, where level set front actually stops, coincident largely with those predicted by (5) in practice. As previously discussed, segmentation result by level set methods based on intensity distribution, require an accurate estimation of intensity distribution, while the global optimum of the estimation is not guaranteed by existing EM methods.

To evaluate the estimation result of intensity distribution, we introduce a probability offset w into equation (5) and define,

$$\phi(x, w) = P_{out}(I(x)) - P_{in}(I(x)) - w, \tag{6}$$

where the boundaries satisfy $E(x, w) = \{x|\phi(x, w) = 0\}$. The value of w indicates the reliability of segmentation results by intensity distribution. For example, a negative w causes the segmentation result of inside region Ω to shrink,

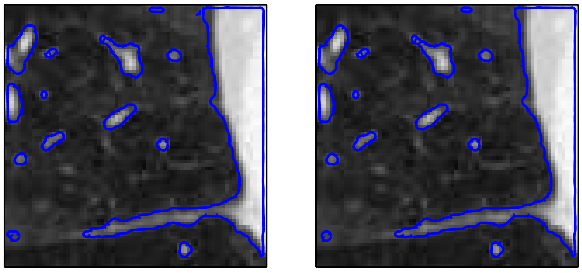

(a) The result of Fig. 1(a) (b) The result of Fig. 1(c)

Fig. 3. Final 3D segmentation results by combining gradient information and intensity distribution on the slice at $z = 10$.

indicating the probability of the inside region Ω has been overestimated. Actually, $\phi(x, w)$ is a hyper-surface similar to the definition of $\psi(x, t)$ in level sets, in which $\phi(x, w) = 0$ represents object boundaries like level sets $\psi(x, t) = 0$ do. Define $d(x, w)$ as the minimum distance from x to object boundaries and the according boundary detector is,

$$Y_e(x, w) = e^{-d^2(x,w)}, \tag{7}$$

where $Y_e(x, w) = 1$ for x on the boundaries and decreases exponentially with distance $d(x, w)$. Different from the intensity-based boundary detector in [2], $Y_e(x, w)$ takes the position x into consideration, indicating voxels in the center of an object are less likely to be boundaries. As we expect the boundaries defined by intensity distribution to overlap with image gradient as much as possible, define an objective function as,

$$S(w) = \int_x (\nabla G_\sigma * I(x)) Y_e(x, w) dx. \tag{8}$$

The global overlap between the boundaries defined by the intensity distribution and gradient is maximized, when

$$\hat{w} = \arg\max_w S(w)\,. \tag{9}$$

Note that existing intensity distribution models assume $\hat{w} = 0$. Furthermore, to adjust boundaries locally, we define a factor $\hat{k}_P = 1 - Y_e(x, \hat{w})$ in the level set speed function representing the boundaries defined by intensity distribution. The final speed factor $\hat{k}$ combining both $\hat{k}_I$ and $\hat{k}_P$ can be designed in many ways. Generally, $\hat{k}$ is assigned a low value when both $\hat{k}_I$ and $\hat{k}_P$ are of low values, and a high value when both $\hat{k}_I$ and $\hat{k}_P$ are of high values. Otherwise, $\hat{k}$ is a balanced value between $\hat{k}_I$ and $\hat{k}_P$. To weight $\hat{k}_I$ and $\hat{k}_P$ automatically, we adopt a fuzzy logic table similar to that in [6].

To find $\hat{w}$ for equation (9), we search scope $[-w_{sc}, w_{sc}]$ in multiple resolutions, and the scope w_{sc} is computed by,

$$w_{sc} = C \cdot \int_u |\frac{P(u) - H(u)}{H(u)}|^2 du \tag{10}$$

where C is an empirical constant and $H(u)$ the normalized histogram at intensity u. Actually, w_{sc} prevents $\hat{w}$ converging

(a) 3D boundary surface reconstructed

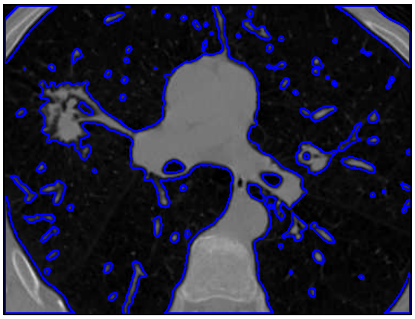

(b) 2D contour on one slice at $z = 26$ in blue lines.

Fig. 4. Segmentation results of a 3D lung image data.

to the boundaries of neighboring objects inside or outside the current object.

The final segmentation results by the proposed method based on the two estimation of intensity distribution in Fig. 1(a) and 1(c) are shown in Fig. 3(a) and 3(b) respectively. The difference between the two results is almost indiscernible. Compared with Fig. 1(b) and Fig. 1(d), some noise in the gradient is filtered out and the right side of the lung wall is preserved well where its gradient is low.

Lin et al. proposed to combine the distribution of both image gradient and intensity [7]. But they did not consider estimation error in intensity and gradient distributions. The advantage of our method is using gradient information to calibrate the instable segmentation results found by level set methods based on instable estimation of intensity distribution. It is helpful especially when the intensity distribution is non-Gaussian, such as Rayleigh or Poisson distribution, where using Gaussian model to estimate the intensity distribution may introduce large estimation error.

IV. EXPERIMENTAL RESULTS AND ANALYSIS

We test the proposed method on a series of CT lung scans downloaded from the National Cancer Institute [8]. A narrow band level set method is implemented to improve speed [1]. Time step is chosen adaptively to satisfy the Courant-Friedrichs-Levy restriction to make segmentation stable. A user only needs to specify a box containing the interested organic structures, or the region of interest (ROI). Using a ROI with $290 \times 380 \times 62$ voxels as the initial front surface, we get the segmentation result with spacing 0.68, 0.68, and 0.63 mm along X, Y, Z axes. To visualize the segmentation

result, we construct a 3D boundary surface using a Marching Cubes (MC) method in [9], as shown in Fig. 4(a). The thin structures like bronchia and fine surface details are well captured. Note that some bronchia are not connected to the major bronchial tree in this part of lungs. This is not resulted from the segmentation or reconstruction error. The 2D contours of the level sets on XY plane are also generated by the MC method, as shown for one slice at $z = 26$ in Fig. 4(b).

From Fig. 4(a) and Fig. 4(b), it is easy to detect a nodule with many connections in the left lung. We can re-assign the ROI to segment the nodule core. Fig. 5(a) and 5(d) show the segmentation results by the intensity distribution on slices at $z = 24$ and 33 respectively. The gradient is shown in Fig. 5(b) and 5(e). Fig. 5(c) and Fig. 5(f) show the segmentation results by the proposed method for comparison. The inside regions of the nodule core were initially underestimated by the intensity distribution, but calibrated by the gradient in the final results as shown by the blue line. To compare with ground truth, we overlap the segmentation results with the manual results by physicians in red contour [8]. From Fig. 5(c) and 5(f), the two contours coincide very well. Note that it is difficult to segment the nodule core by gradient information alone since the gradient around the nodule core is not distinctive from that around the outline of the nodule.

In the experiments, we find that final segmentation results are decided largely after the global calibration by $\hat{w}$, indicating the role of local adjustment by the fuzzy logic table is limited. In other words, $\hat{w}$ causes the boundary defined by intensity distribution to shrink or expand globally to overlap with image gradient as much as possible, which is essential to make final segmentation results stable. Nevertheless, the proposed method can not "correct" segmentation results when the SEM method gives an estimation of intensity distribution that largely deviates from the true distribution. In practice, we run SEM method several times to select the best estimation with the minimal w_{sc} value.

The estimation of intensity distribution of the ROI with $290 \times 380 \times 62$ voxels takes about 29 seconds while the level set segmentation takes 15 minutes. Our experiments are carried out on an AMD Athlon64 3700 processor with 1G RAM. The algorithm has been run automatically over a total of 23 data sets and the results have been validated by experienced physicians. Quantitative evaluation will be conducted in the near future for the purpose of nodule classification.

V. CONCLUSION AND FUTURE WORK

In this paper we propose a new mechanism to combine gradient information and intensity distribution into level set speed function. Intensity distribution based level set methods only give instable segmentation results on low-intensity medical structures, due to instable estimation of intensity distribution. Using gradient information to calibrate the intensity distribution based segmentation results, the proposed method tolerates estimation errors of intensity distribution. It filters out some noise and preserves object boundaries with low gradient. Experimental results show the proposed method can generate stable and accurate segmentation results for complex organic structures like lung bronchia and nodules. In the future we want to (1) combine shape information in segmenting specific structures; (2) and automatically classify malignant and benign nodules based on the their geometric features.

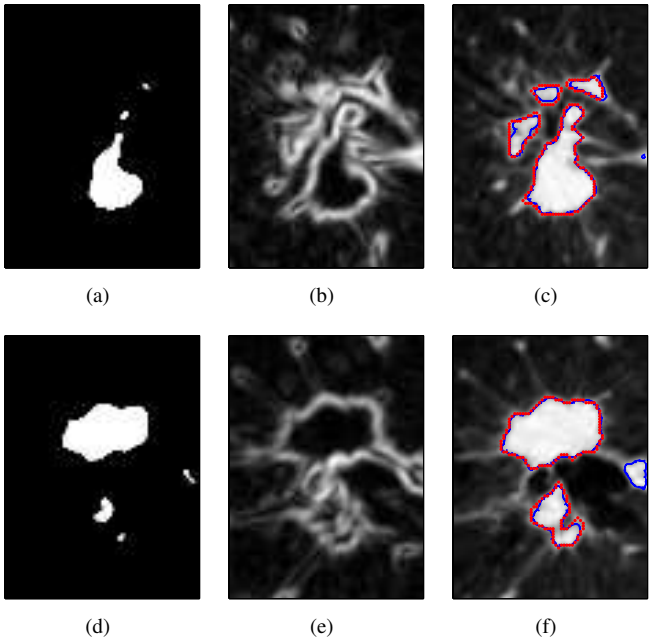

Fig. 5. Segmentation results on nodule slices at $z = 24$ and 33. (a) and (d) are the segmentation results by intensity distribution; (b) and (e) are the gradient; And (c) and (f) are the final result by the proposed method in **blue** lines. The **red** lines are the nodule cores manually marked by physicians.

REFERENCES

[1] R. Malladi, J. A. Sethian, and B. C. Vemuri, "Shape modeling with front propagation: A level set approach," *IEEE Transactions on Pattern Analysis and Machine Intelligence*, vol. 17, no. 2, pp. 158–175, Feb 1995.

[2] C. Baillard, C. Barillot, and P. Bouthemy, "Robust adaptive segmentation of 3d medical images with level sets," INRIA, Tech. Rep. RR-4071, 2000.

[3] A. Dempster, N. Laird, and D. Rubin, "Maximum likelihood from incomplete data via the EM algorithm," *Journal of Royal Statistical Society*, vol. 3, pp. 1–38, 1976.

[4] A. Tsai, W. Wells, S. Warfield, and A. Willsky, "Level set methods in an EM framework for shape classification and estimation," in *MICCAI (1) 2004*, 2004, pp. 1–9.

[5] P. Masson and W. Pieczynski, "SEM algorithm and unsupervised statistical segmentation of satellite images," *IEEE Transactions on Geoscience and Remote Sensing*, vol. 31, no. 3, pp. 618–633, 1993.

[6] C. Ciofolo, C. Barillot, and P. Hellier, "Combining fuzzy logic and level set methods for 3D MRI brain segmentation," in *IEEE International Symposium on Biomedical Imaging (ISBI)*, 2004, pp. 161–164.

[7] P. Lin, C.-X. Zeng, Y. Yang, and J.-W. Gu, "Statistical model based on level set method for image segmentation," in *The Fourth International Conference on Computer and Information Technology*, 2004, pp. 143–148.

[8] "Lung Image Database Consortium (LIDC) Materials," http://imaging.cancer.gov/reportsandpublications/ReportsandPresentations/LungImaging, National Cancer Institute.

[9] S. Liu and J. Li, "Surface construction using tricolor marching cubes," in *International Conference on Computer Graphics Theory and Applications*, 2006.